

pubs.acs.org/Macromolecules Article

Kinetics of Polymer Gel Formation Cause Deviation from Percolation Theory in the Dilute Regime

Haley K. Beech, Tzyy-Shyang Lin, Devosmita Sen, Dechen Rota, and Bradley D. Olsen*



Cite This: Macromolecules 2023, 56, 9255-9263



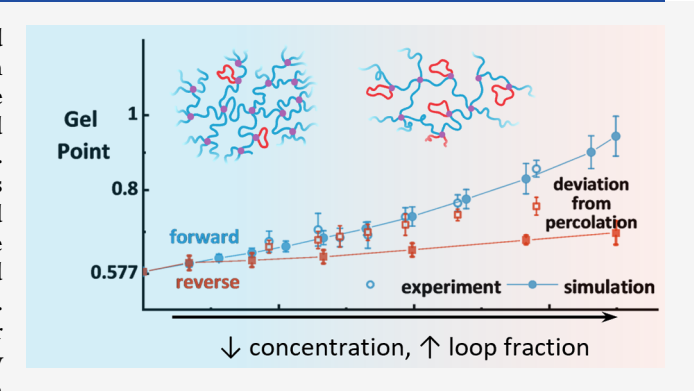
ACCESS I

Metrics & More

Article Recommendations

s Supporting Information

ABSTRACT: Gelation has long been conceptualized and modeled as a percolation process in which bond formation or destruction events are random. Percolation assumes that connections are created or destroyed randomly such that the critical point should occur at the same point when approached from either direction. Here, the gel point of an end-linked poly(ethylene glycol) gel was measured during forward (bond forming) and reverse (bond breaking) gelation and degelation processes to interrogate how the gel point scales with synthesis concentration, where decreased concentration leads to an increased prevalence of inelastic loops. Forward gel points, measured with combined kinetic nuclear magnetic resonance (NMR) and diffusing wave spectroscopy (DWS) experiments, were identical to results generated from a



kinetic Monte Carlo (KMC) simulation, demonstrating the expected gel point suppression as the concentration decreased. Reverse gel points, measured with a selective degradation technique, were within the error of forward gel points at high concentrations but displayed a lesser degree of suppression as the concentration decreased. This deviation between forward and reverse gel points at low concentrations was qualitatively reproduced in the KMC simulation. These experiments and simulations show that forward and reverse gel points diverge as the gel system becomes more dilute, suggesting that kinetic effects cause a departure from the percolation behavior in defect-rich gels.

INTRODUCTION

Accurately predicting and quantifying the gel point is extremely important for many applications ranging from reactive extrusion^{1,2} to injectable hydrogels for drug delivery.³ In a chemically cross-linked system, the transition from viscoelastic fluid to solid occurs when the number of cross-links reaches a critical threshold, at which point the weight-average molar mass diverges. This sol-gel transition has traditionally been understood in analogy to the theory of percolation. 4-7 Cross-linker molecules are considered sites on a lattice, and the formation of cross-links is viewed as the formation of bonds between sites. When bonds are formed at random, the critical transition from disparate connections to a percolated network (Figure 1) occurs at a critical fraction of bonds p_o , which is a specific value of the bond formation probability, p. Bond formation requires that both ends of the polymer linker react with a cross-linker; individual reaction events are tracked by the chemical conversion, q, where $q^2 = p$ for random bonding (Figure 1a).

Around the sol—gel transition, the material behavior changes rapidly; properties such as weight-average molecular weight and viscosity diverge as the distance between p and p_c becomes small. It is therefore desirable to be able to predict the conversion at which this transition will occur, but the percolation threshold depends on both dimensionality and lattice type (Figure 1b,c) and is notorious for being challenging to accurately quantify.⁸

Percolation theory assumes that the bond formation probability is independent of the size and structure of reacting molecules but requires bonds to form between adjacent vertices on a lattice. The widely used Flory—Stockmayer gelation theory, also known as the mean-field approach, is percolation on a Bethe lattice with infinite dimensionality (Figure 1d). Percolation theory recovers the Bethe lattice prediction at and above six dimensions. Indeed, Flory—Stockmayer theory is still widely acclaimed because it is the classical result that is recovered whenever intermolecular connections between any two reactive groups not connected to the same molecule are made with equal probability, regardless of their position, which molecule they belong to, and whether or not a lattice is used. 13

The example lattices in Figure 1b,1c depict bond percolation, but other forms of percolation are also commonly applied to gelation. Bond, site, and site-bond are all lattice-based percolation theories and as such all invoke the assumption of

Received: May 2, 2023
Revised: October 25, 2023
Accepted: October 26, 2023
Published: November 14, 2023





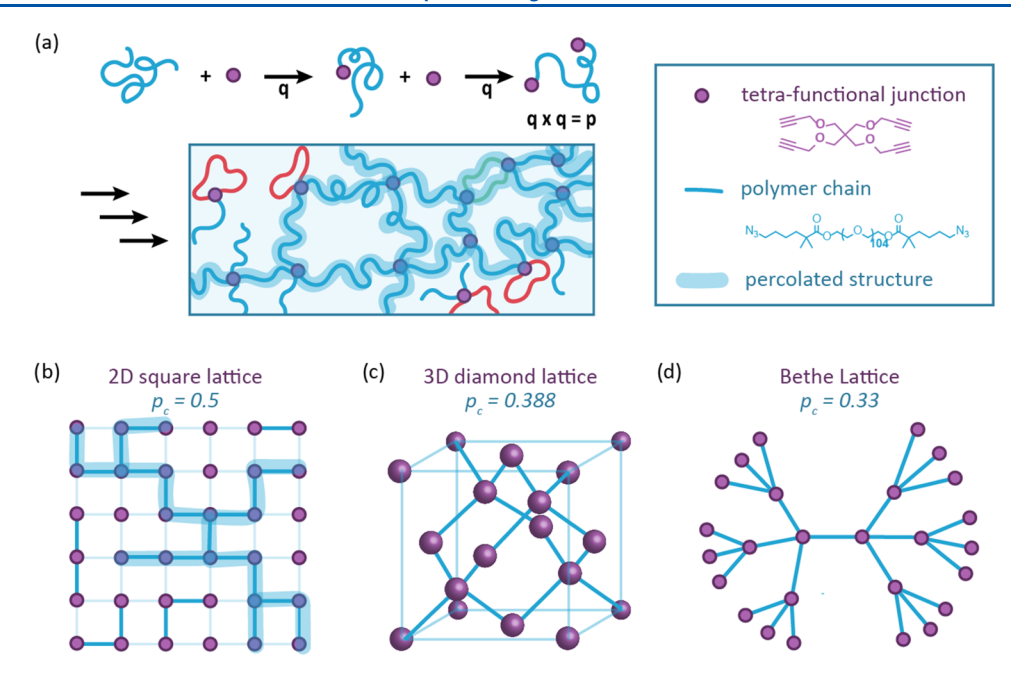


Figure 1. (a) End-linking reactions lead to the emergence of a percolated polymer network. Lattices composed of tetrafunctional junctions in 2D, 3D, and an infinite dimensional Bethe lattice (b-d) respectively. The critical percolation threshold, p_{σ} is given for each.

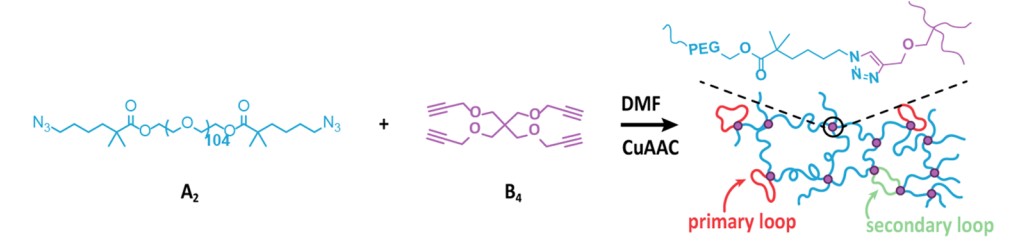


Figure 2. Chemical synthesis of the tetrafunctional PEG gel via copper-catalyzed alkyne azide click chemistry. The synthesis resulted in gels with known primary and secondary loop fractions.

random placement of the bonds, sites, or both, respectively. Bond and site percolation have different percolation thresholds, with bond percolation typically applied to melt or concentrated systems and site more commonly applied to dilute gel systems. ^{4,8,14} Site-bond percolation sets both the bond and site occupation probabilities independently and has previously been employed to look at concentration-determined percolation as opposed to time-based reactive gelation. ^{15,16} The assumption that any two occupied sites next to each other are bonded is not physically translatable to an end-linked network, and as such, site percolation is more readily applied to gelation through the polymerization of multifunctional monomers. ¹⁷

In discussing different types of percolation, it is important to distinguish between topological and kinetic effects. One key difference between percolation on a lattice versus in an experiment is the nonideal topological connectivity that constitutes the tangible network. Recent studies on the gelation of end-linked gels have shown that topological defects such as loops lead to gel point suppression, a phenomenon that is dependent on the preparation condition of the precursors as well as the ultimate topology of the cross-linked network. Furthermore, the translation from a real polymer network to a well-defined lattice (Figure 1a versus c or d) is an approximation that neglects topological complications such as a broad distribution of loop orders. Whether such factors affect only the numerical value of the gel point or actually disrupt the critical

behavior predicted by the percolation theory is still largely unknown. Prior work is inconclusive; while many authors have studied the critical behavior of networks and report agreement with 3D percolation predictions, ^{22–25} others report a transition from mean field to 3D, ²⁶ while others report exponents which do not agree with either. ^{27–29} Topological effects should impact both the forward and reverse measurements to the same extent and can be varied in percolation theory by changing the lattice or type of percolation. Kinetic effects are concerned with the relative rates of formation of different topological structures such as loops, branches, and elastically effective strands. If these rates change throughout the course of the experiment, indicating correlated events, then the core randomness assumption is violated and any lattice-based percolation theory no longer applies unless a correlated probability is considered; this could in turn change the critical behavior of the system.^{4,30} This possibility of kinetic effects that cause deviation from random bond or site placement is tested here

In this work, the physics of the sol—gel transition is examined through the study of the gelation of an end-linked system prepared by cross-linking a stoichiometric amount of bifunctional polymeric precursors with small molecule tetrafunctional cross-linkers (structures shown in Figure 1). Symmetry is an intrinsic property of a noncorrelated percolation process; if bond formation is truly random, the transition should occur at the same point regardless of the direction of approach.

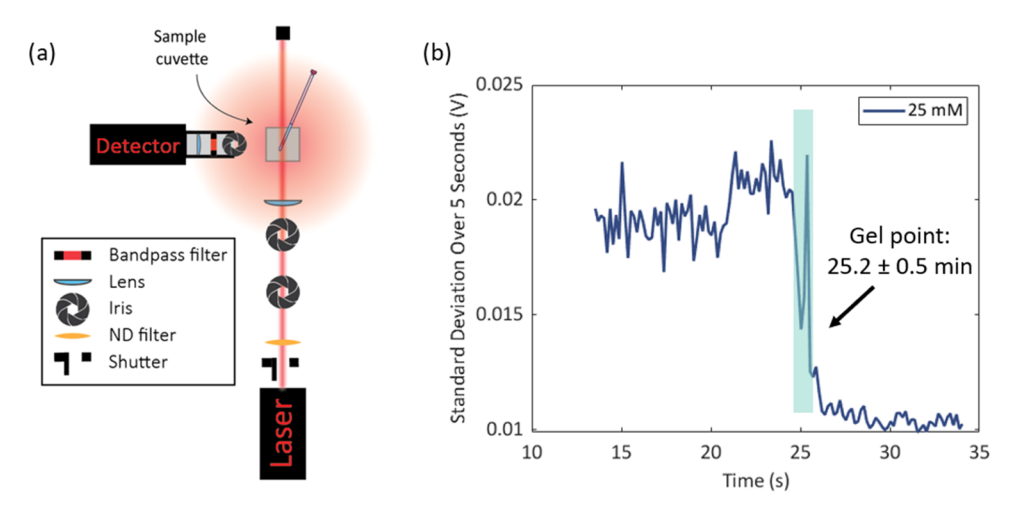


Figure 3. (a) Diffusing wave spectroscopy set up built to measure the time at which the gel point occurred during network formation. (b) Representative light intensity variance data from the DWS used to determine the gel point.

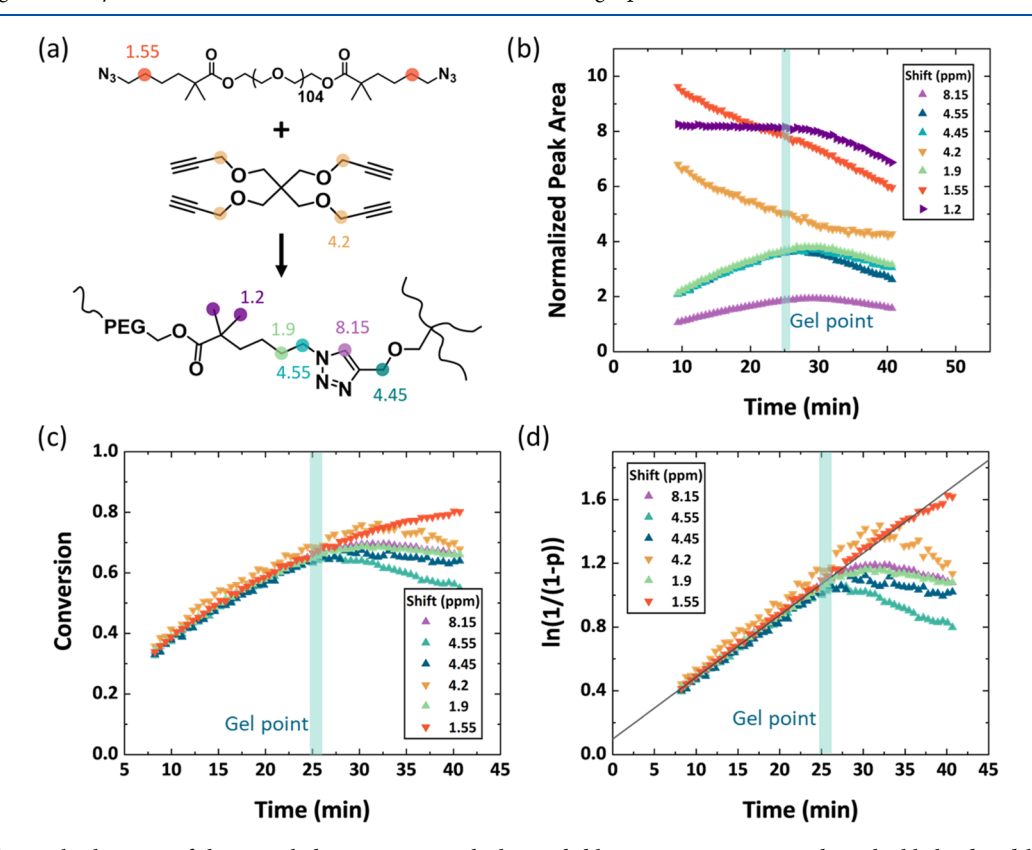


Figure 4. (a) Chemical schematic of the cross-linking reaction with the trackable proton-containing carbons highlighted and labeled with their downfield shifts. (b) NMR peak integration normalized by the solvent peak over the time course of the gelation reaction. Kinetic data are accurate up to the gel point, after which the sample becomes a viscoelastic solid, and quantitative integration becomes unreliable. (c) Calculated conversion as a function of time. (d) Linearized conversion data demonstrate pseudo first-order kinetics, as expected for the CuACC reaction. Data are shown for the 25 mM mixed degradation sample.

Comparing forward to reverse gel point measurements across a range of polymer gel concentrations will further elucidate the applicability of percolation theory.

■ EXPERIMENTAL APPROACH

Experiments were carried out on a bifunctional azide-terminated poly(ethylene glycol) (PEG, MW = 4600 g/mol, N = 36, $b = 1.1 \text{ nm})^{31}$ system cross-linked with a tetrafunctional alkyne small molecule via copper-catalyzed azide alkyne cycloaddition (CuAAC) in N,N-dimethylformamide (DMF) at varied PEG precursor concentrations,

as shown in Figure 2. The topology of this network has been previously studied with network disassembly spectrometry, leading to a detailed understanding of the dependence between the dimensionless concentration and loop formation. $^{32-34}$ The overall network topology can be controlled by a single dimensionless parameter, cR^3 , where c is the concentration of the bifunctional precursors and R denotes the rootmean-square end-to-end distance of the linear precursor, assuming an unperturbed Gaussian chain. The dimensionless parameter is the product of the macromer concentration and the pervaded volume of each macromer chain that represents the ratio between the intramolecular length scale and the intermolecular length scale. When the

parameter is large, intermolecular branching reactions dominate, and the resulting network is mostly free of small loops. On the contrary, when the parameter is small, intramolecular looping reactions become significant, and abundant loops are found within the fully cross-linked network. Gels were synthesized at 8, 10, 12, 14, 16, 18, and 25 mM initial polymer concentration ($cR^3 = 0.69-2.14$), corresponding to primary loop fractions of 0.33–0.09 over that same range.

Forward Gel Point Quantification. The forward gel point was measured with a combination of diffusing wave spectroscopy (DWS) and proton nuclear magnetic resonance (¹H NMR) to monitor the dynamic sol to gel transition and conversion simultaneously. DWS is a light scattering method that accounts for multiple scattering, making it ideal for gels. 36-38 Experiments were conducted on a home-built DWS with a custom NMR tube sample holder (Figure 3a), as detailed in the Diffusing Wave Spectroscopy section of SI. Microparticles were added to the gel samples at a loading of 0.5 wt % such that the majority of the scattering signal (~95%) was from particles (Figure S1). Control experiments showed that the moduli of the gels were unaffected by particle size (Figure S2), and the conversion of the gel point was unaffected by particle size, particle loading, catalyst loading, or degradable strand content (Figure S3). The 1-µm diameter particles were selected to be significantly larger than the mesh size, quantified as average correlation length measured via small angle neutron scattering to be in the $1-10~\rm nm$ range. The particles therefore became trapped when the incipient gel formed. The dynamics of the microparticles were captured in the light scattering signal; the incipience of a gel dampened particle dynamics, leading to smaller fluctuations, as demonstrated in the standard deviation of the light intensity plotted in Figure 3b. Details of this quantification are included in Section 2d of the SI, but the transition was generally visually apparent in the data and occurred over a less than a 1 min window.

Kinetic NMR data were used to determine the conversion up to the gel point. Previous work has shown that quantitative measurements on gelling systems are accurate until gelation in the pregel regime. 41,42 In the chemical system, there are 4 appearing peaks and 2 disappearing peaks, which are tracked to measure conversion, corresponding to the protons marked and labeled with their downfield shifts in Figure 4a. An analysis of the ${}^{1}H$ NMR spin-lattice relaxation constant, T_{1} , was used to ensure an accurate quantitative integration. Based on the relaxation analysis (SI Section 2b), a single 4 s scan was collected every 30 s to track conversion. Peak areas were normalized with the solvent peak area and internally against a constant methyl peak (Figure 4b) and were also validated with a tetramethylsilane (TMS) standard addition (SI Section 2c). Once normalized, the conversion over time was calculated for each of the 6 peaks, as shown in Figure 4c. The conversion data track together until after the gel point (as measured by DWS), at which point the signal starts to dampen due to extremely fast proton relaxation. The data were linearized according to pseudo first-order kinetics, shown in Figure 4d, which have been shown to apply for CuAAC reactions. 43 The linearity is maintained until slightly past the gel point, confirming the validity of the conversion quantification. The conversion at the gel point was extracted from the NMR data by using the time at which gelation was observed in the DWS data.

Reverse Gel Point Quantification. The reverse gel point was measured by synthesizing two different azido-functionalized end groups, one degradable and one nondegradable in basic conditions as shown in Figure 5a. A series of samples with varying degradable content was synthesized at each concentration, tested to ensure no significant variation in moduli as a function of degradable content (Figure S4), and then degraded with 1.5 M KOH. Samples were monitored and allowed to equilibrate for 2 days before measurement; no further changes were observed for over a week after the initial equilibration period. The gel point could be identified visually by looking at the state of the gel; a 2% difference in degradability content created a notable transition from a macroscopic piece of gel to a homogeneous solution. The depercolation threshold was defined as the transition between a clear solution with a solid gel to a liquid solution with suspended microparticles and no macroscopic piece that could be filtered out, as shown in Figure 5b (data in SI Section 3d). Microparticles were included because they were used in the DWS measurement to quantify the gel point; here, the

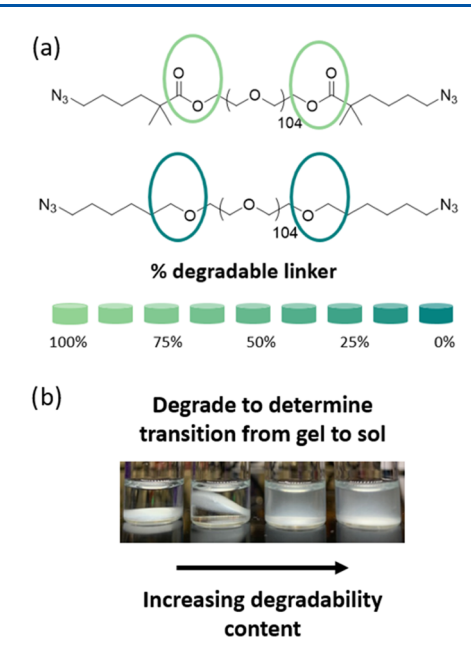


Figure 5. (a) Degradable and nondegradable macromers used to synthesize a series of gels with varied degradable content. (b) Representative visual data of the reverse gel point measurement.

indicator was when they were released from the gel, as opposed to when they became trapped within the gel. These measurements were repeated across gel concentrations to collect reverse gel point data as a function of loop defects.

Kinetic Monte Carlo Simulation. Forward and reverse gel points were also predicted with a kinetic Monte Carlo (KMC) simulation by tracking the cluster size distribution during network growth and dissolution. The KMC algorithm from the experimentally validated simulation procedure first developed by Stepto and co-workers ^{44–47} and later revised by Olsen and co-workers ^{33,34,48,49} was adopted. This simulation employs a reaction-limited assumption, where the diffusion of the reactants and chain relaxation are much faster than the reaction rate. This assumption has been shown to apply over a wide concentration range in the end-linking process, ⁵⁰ and importantly, allows the spatial location of polymer segments and junctions to be neglected, enabling a large system size of up to 40,000 chains. In the simulation, the propensities for the reactions between all pairs of unreacted sites were tracked and re-evaluated at each simulation step according to the reaction probability relation

$$P_{\rm AB} \propto \frac{1}{V} + \left(\frac{3}{2\pi R^2 d_{\rm AB}}\right)^{3/2} \tag{1}$$

where V is the volume of the reactor and d_{AB} is the shortest topological distance (number of bifunctional precursors found on the shortest path) between a chain A and cross-linker B. The 1/V term in eq 1 represents the pairwise concentration of any pair regardless of the surrounding network that determines the probability for contact, while the second term represents a pair's internal concentration if the two groups are connected to the same network that determines the looping probability of a connected path d_{AB} . Based on this probability, an unreacted chain and an unreacted cross-linker are selected at each reaction step. If the two selected groups are not connected before the reaction, d_{AB} is infinite and the reaction results in an intermolecular connection. If the two selected groups are connected, d_{AB} is a finite number x and the reaction results in an intramolecular connection and the number of xth order loops increases by one, where x is the number of chains in the loop. The cluster sizes of connected components and the shortest distances between chain-cross-linker pairs are updated after a selected A - B pair reacts. The KMC simulation accurately predicts primary and secondary loop fractions in end-linked PEG gels.

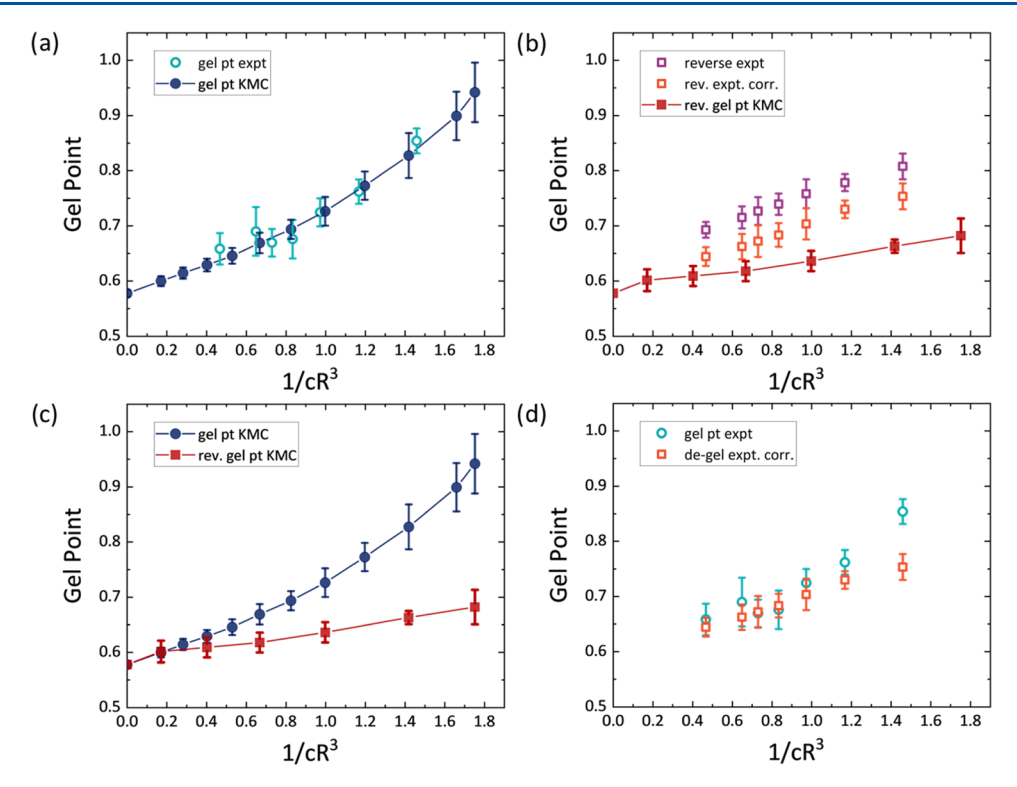


Figure 6. (a) Conversion at the forward gel point from combined DWS/NMR measurements agrees with KMC gel point data. (b) Conversion at the reverse degel point from selective degradation measurements was systemically greater than those predicted by KMC. Experimental measurements were corrected to account for the actual conversion achieved in nondegradable PEG macromer synthesis. KMC error is from the uncertainty in extrapolation to infinite system size. (c) Simulation predicts a deviation between forward and reverse gelation. (d) Experimental forward and reverse gel point data deviate as the system becomes dilute.

At the gel point, the weight-average molecular weight of the system diverges as an infinite molecule forms. Due to computational system size limitations, this divergence is not captured cleanly in simulation. Instead, the reduced molecular weight, or the weight-average molecular weight of all clusters excluding the largest, is used to determine the gel point. 18,35,45,51 The reduced molecular weight exhibits a sharp peak at the system gel point, as shown in Figure S23 in SI. The gel point of KMC systems with a varying number of chains ranging from 15,000 to 40,000 was calculated and extrapolated to an infinite system size as detailed in Section 4a of the SI. Simulations were performed with the following parameters: Kuhn length b = 1.1 nm, number of Kuhn segments N = 36, and dimensionless concentrations from $cR^3 = 0.57$ – 5.85 for comparison to experiments. For the reverse gelation, the networks obtained from the forward gelation were sequentially dismantled by randomly breaking a discrete percentage of network strands. After each breaking step, the weight-averaged molecular weight and reduced molecular weight of the clusters were calculated. Plotting the reduced molecular weight as a function of percentage of broken strands (Figure S25) generates data similar to the forward reaction calculation, where the depercolation threshold is extracted as the peak in the reduced molecular weight plot. The codes used for forward and reverse gel point calculations are available in the GitHub repository linked in ref 52.

■ RESULTS AND DISCUSSION

Gel point results are first compared to examine the agreement with theory and then to analyze the forward and reverse behavior. Forward gel points from coupled kinetic experiments and KMC simulations at different dimensionless synthesis concentrations were in close agreement, as shown in Figure 6a. All measured gel points were within error of the KMC results; the simulation data were also previously shown to be in good agreement with gel point data collected by Wile (reported by

Spouge), ⁵³ Gordon and Scantlebury, ⁵⁴ and Cail and Stepto, ⁵⁵ as reported by Wang et al. ¹⁸ When the system is loop-free, a scenario only achievable in simulation, the Flory–Stockmayer gel point $q_c = (f-1)^{-0.5} \approx 0.577$ is recovered as expected for a model in which connections between any two reactive groups are made with equal probability. As the loop content increases $(1/cR^3$ increases), the onset of forward gelation is delayed. The simulation has no fitting parameters and is in close agreement with the experimental PEG gel data, which have been measured previously with NDS, directly demonstrating the importance of intramolecular reactions in predicting the gel point. This suggests that a purely topological model, neglecting diffusion, packing, entanglement, and compositional fluctuations, is adequate for quantitative prediction of the gel point in end-linked networks.

Reverse gel points from gel degradation experiments and KMC simulations exhibit less extreme gel point delay than the forward measurements, as demonstrated in Figure 6b. Here, the original degel data from experiments lies above the measurements predicted by KMC. The experimental data are not as closely aligned with the KMC simulation results as in the forward measurement, although both exhibit less drastic gel point suppression at low concentrations.

The reverse gel point experiment is sensitive to incomplete conversion during the forward reaction steps because every chain that is not elastically effective counts as an extra link that is cleaved, biasing the measurement toward a lower number of degradable bonds. Analysis of precursor NMR traces in the SI (Section 2f) shows that the conversion of the functional group coupling reaction for the nondegradable prepolymer was ~93%, which causes a systemic bias in the recorded data because 7% of

reactive groups were not actually active. When this is accounted for (SI section 3e), the experimental gel point data are shifted to slightly lower values. While this bias is directly accounted for in the efficiency correction above, the degradable PEG functionalization reaction and the click reaction itself are also limited by imperfect chemical conversion. Even the very high conversions (>98%) supported by NMR and FTIR data in the SI are imperfect and compounding. This effect is minimally impactful in forward gelation because the conversion is only tracking bonds that successfully form before the gel point without regard for groups that remain unreacted at the end. The degradable content of the network did not have an impact on the forward gel point, as gels made with 100% degradable and a 50/50 mixture of degradable/nondegradable PEG had the same conversion at the gel point (Figure S3a).

Forward and reverse gel points from the simulation and experiment are directly compared in Figure 6c,d, respectively. It is observed that for systems with small loop contents (low 1/ cR^3) the gel points of the forward and reverse gelation are within error, indicative of a symmetric, percolation-like behavior. However, for systems with larger loop contents, the gel points between the two sets become disparate, and significant hysteresis can be observed between the forward and reverse gelation, breaking the symmetry between the two processes. The difference between forward and reverse gel point measurements at the $cR^3 = 1.45$ data point is significant with a student's twotailed t test α < 0.01, or with 99% certainty, while the difference at $cR^3 = 1.18$ is significant with a student t test $\alpha < 0.1$, or with 90% certainty, which does suggest a divergence considering the prior points have no significance. Where this divergence begins to occur differs between simulation and experiment: $1/cR^3 > 0.4$, primary loop fraction >15% in simulation, while the divergence is later, at $1/cR^3 > 1.2$ and a primary loop fraction >25% in the experiment. Previous work by Sakai et al. similarly found that the fractal dimension of percolation clusters in a tetra-PEG system began to deviate away from the lattice-based percolation prediction when $1/cR^3$ was greater than one. 15

Regardless of where the forward/reverse deviation occurs, the hysteresis is captured in the scaling of gel point delay with dimensionless concentration, as plotted in Figure 7. The relationship $\Delta p = (p_{\rm actual} - p_{\rm ideal}) \sim (cR^3)^{-\alpha}$ yields $\alpha_{\rm forward} = 1.18 \pm 0.05$ while $\alpha_{\rm reverse, expt.} = 0.88 \pm 0.03$ and $\alpha_{\rm reverse, KMC} = 0.64 \pm 0.08$ for the data presented in Figure 7. These are all within the

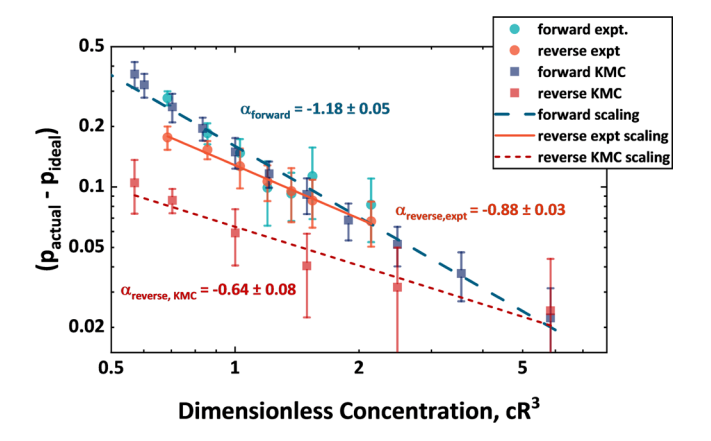


Figure 7. Scaling of the deviation from the ideal gel point with dimensionless concentration yields significantly different exponents for the forward and reverse process. Decreasing cR^3 correlates with increasing loop fraction, as shown in prior literature. ^{33,34,57}

range of exponents reported from a variety of previous works measuring the forward gel point (α = 0.63 to 1.36) across many different chemical systems, and the forward gel point α unsurprisingly matches the data sets which were reported above to agree with the KMC simulation, which all have α > 1. 19,53-56 The difference in α within a single chemical system is evidence toward a deviation from percolation behavior.

One possible explanation often employed for the departure from classical percolation is diffusion effects, which often manifest in diffusion-controlled off-lattice models, such as monomer-cluster or cluster-cluster aggregation. ^{19,58-60} Lang and Müller recently presented a diffusion-limited gelation simulation that considers the dynamics and conformations of the molecules in space and reported a scaling exponent of $\alpha \le 2$ 3. They summarized many previous gel point studies, the majority of which report $\alpha > 1$ when all data points are included in the fit, but they are discounted due to unequal reactivity. This means that the gel point deviation is scaling more quickly than anticipated because different reactive groups have different probabilities of reacting, which could be due to a large number of effects including diffusion limitations, steric hindrance, or topological constraints. However, the gel synthesis reaction used here and most solution-based reactions are not diffusioncontrolled for a vast majority of gelation reactions based on prior experimental work⁵⁰ and Damköhler number analysis.³⁹ As Dušek sagely points out in his review of gelation behavior, diffusion in gel formation is a seemingly contradictory scenario: while network formation will always pass through a stage when the process is diffusion-controlled, the structure evolution in many systems is practically unaffected by diffusion over a wide range of conversions. ¹³ So, although it is possible that the abrupt increase in viscosity at the gel point causes diffusion effects to become important, the agreement between a variety of gel point data sets and the reaction-limited KMC simulation here suggests that the gelation process is largely unaffected by diffusion limitations.

It therefore seems likely that the large degree of forward gel point suppression is caused by unequal reactivity stemming from topological, not diffusional, kinetic constraints. In the KMC simulation, the propensity for a given reaction is directly dependent on whether two groups form a bridge or a loop when reacted. As shown in eq 1, the probability of reaction depends inversely upon the topological distance d_{AB} between two groups such that two groups that are topologically close to each other have a slightly higher chance of reacting, generating a loop. In the semidilute and higher concentration regime, where branching reactions are favored, loops are less abundant and the forward gel points align with reverse gel point measurements. However, as the concentration decreases and the primary loop fraction at full conversion becomes substantial, the forward gelation diverges from the behavior of the truly random reverse gel point. Looping events are favored, and abundant looping events occur before the onset of the sol-gel transition. Since looping events do not contribute to the growth of the overall molecular weight, they significantly delay the onset of gelation and may lead to the large values measured for the α scaling exponent.61

Returning to the original percolation problem, a relatively wide range of the concentrations tested here follow the classical percolation behavior, as supported by the agreement between experimental forward and reverse gel point measurements. The agreement in the experimental system suggests that while topological loops and defects cause gel point suppression, the

propensity for looping changes relatively little as a function of conversion. This is supported by previous measurements of loop fractions measured with NDS and rate theory over the course of the gelation reaction, which showed a relatively constant rate of loop formation at a semidilute concentration. Stated another way, the odds that a particular strand forms a loop during gel formation are equivalent before and after the gel point in the regime where loops are present but are not highly correlated, shown schematically on the left in Figure 8. When the forward

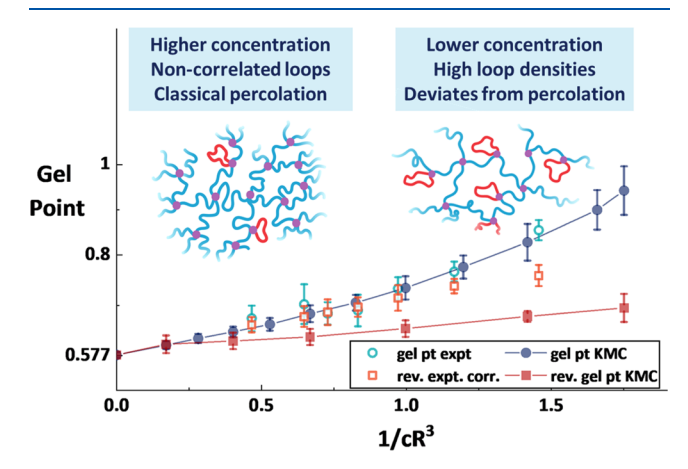


Figure 8. Comparison of forward and reverse gel point measurements with characteristics of the high- and low-concentration gels shown schematically. High concentration networks correspond to the schematic representation of the network, which resembles the Bethe lattice used in Flory–Stockmayer theory with isolated defects. Lower concentration gels correspond to the representation with a high level of defects.

and reverse gel points begin to diverge is indicative of unequal reaction propensity over the course of the reaction. This occurs when the gel concentration becomes dilute and loops become correlated, as shown on the right in Figure 8. Because the odds of selecting a loop to cut during gel dissolution are always equivalent, the deviation suggests that the kinetics of gel formation are causing the additional gel point suppression.

In summary, this work provides simulation and experimental studies on the gelation of end-linked networks to interrogate the adherence to critical percolation behavior. When the system predominately favors branching reactions over looping reactions, the gelation, both forward and reverse, closely traces the Flory-Stockmayer theory predictions corrected for loops and the mean-field percolation provides a fitting description for the gelation behavior. However, when the relative rate of looping reactions is increased, the system not only experiences changes in the loop content at full conversion but also experiences a qualitatively different transition near the gel point, as indicated by the divergence of the forward and reverse gel point as the gel synthesis concentration decreased. Overall, the evidence suggests that the classical analogy between gelation and critical percolation does align with the majority of the semidilute gelation data presented here. As the gel preparation conditions become dilute and topological defects become more prevalent, the sol-gel transition can deviate from the classical picture. In the dilute regime, additional physics, such as variable or correlated rates of loop formation, should be considered to obtain more accurate descriptions of this complex phenomenon.

ASSOCIATED CONTENT

Supporting Information

The Supporting Information is available free of charge at https://pubs.acs.org/doi/10.1021/acs.macromol.3c00831.

Chemical synthesis and characterization data; diffusing wave spectroscopy validation; kinetic NMR controls and analysis; reverse gel point measurement analysis; and kinetic Monte Carlo simulation details (PDF)

AUTHOR INFORMATION

Corresponding Author

Bradley D. Olsen – Department of Chemical Engineering, Massachusetts Institute of Technology, Cambridge Massachusetts 02139, United States; oorcid.org/0000-0002-7272-7140; Email: bdolsen@mit.edu

Authors

Haley K. Beech – Department of Chemical Engineering, Massachusetts Institute of Technology, Cambridge Massachusetts 02139, United States; orcid.org/0000-0003-3276-8578

Tzyy-Shyang Lin — Department of Chemical Engineering, Massachusetts Institute of Technology, Cambridge Massachusetts 02139, United States; orcid.org/0000-0002-8265-6702

Devosmita Sen — Department of Chemical Engineering, Massachusetts Institute of Technology, Cambridge Massachusetts 02139, United States

Dechen Rota — Department of Chemical Engineering, Massachusetts Institute of Technology, Cambridge Massachusetts 02139, United States

Complete contact information is available at: https://pubs.acs.org/10.1021/acs.macromol.3c00831

Notes

The authors declare no competing financial interest.

■ ACKNOWLEDGMENTS

This work was supported by the NSF Center for the Chemistry of Molecularly Optimized Networks (MONET), CHE-2116298. We would like to thank John Grimes and Dr. Walt Massefski at the Department of Chemistry Instrumentation Facility at MIT for their expertise in kinetic NMR data collection and analysis.

REFERENCES

- (1) Tellers, J.; Pinalli, R.; Soliman, M.; Vachon, J.; Dalcanale, E. Reprocessable Vinylogous Urethane Cross-Linked Polyethylene via Reactive Extrusion. *Polym. Chem.* **2019**, *10* (40), 5534–5542.
- (2) Zou, W.; Tupper, A.; Rebello, N. J.; Ranasinghe, D. S.; Green, W. H.; Couch, C.; Olsen, B. D. Multiscale Modeling and Characterization of Radical-Initiated Modification of Molten Polyolefins. *Macromolecules* **2022**, *55* (14), 5901–5915.
- (3) Hoare, T. R.; Kohane, D. S. Hydrogels in Drug Delivery: Progress and Challenges. *Polymer* **2008**, 49 (8), 1993–2007.
- (4) Stauffer, D.; Coniglio, A.; Adam, M. Gelation and Critical Phenomena. *Adv. Polym. Sci.* **1982**, 44, 103–158.
- (5) Djabourov, M. Gelation—A Review. Polym. Int. 1991, 25 (3), 135–143.
- (6) Djabourov, M.; Nishinari, K.; Ross-Murphy, S. B. The Sol-Gel Transition. *Phys. Gels Biol. Synth. Polym.* **2013**, 64–96.
- (7) Hammersley, J. M. Percolation Processes. *Math. Proc. Cambridge Philos. Soc.* **1957**, 53 (3), 642–645.

- (8) Stauffer, D.; Aharony, A. Introduction to Percolation Theory, 2nd revised ed.; Taylor & Francis Inc.: Philadelphia, 1994.
- (9) Stockmayer, W. H. Theory of Molecular Size Distribution and Gel Formation in Branched-Chain Polymers. *J. Chem. Phys.* **1943**, *11* (2), 45–55
- (10) Stockmayer, W. H. Theory of Molecular Size Distribution and Gel Formation in Branched Polymers. II. General Cross Linking. *J. Chem. Phys.* **1944**, *12* (4), 125–131.
- (11) Flory, P. J. Molecular Size Distribution in Three Dimensional Polymers. I. Gelation. *J. Am. Chem. Soc.* **1941**, *63*, 3083.
- (12) Hiemenz, P. C.; Lodge, T. P. Polymer Chemistry; CRC Press: Boca Raton, FL, 2007.
- (13) Dušek, K. Diffusion Control in Kinetics of Cross-Linking. *Polym. Gels Networks* **1996**, *4*, 383–404.
- (14) Tsuji, Y.; Nakagawa, S.; Gupit, C. I.; Ohira, M.; Shibayama, M.; Li, X. Selective Doping of Positive and Negative Spatial Defects into Polymer Gels by Tuning the Pregel Packing Conditions of Star Polymers. *Macromolecules* **2020**, *53* (17), 7537–7545.
- (15) Sakai, T.; Katashima, T.; Matsushita, T.; Chung, U. Il. Sol-Gel Transition Behavior near Critical Concentration and Connectivity. *Polym. J.* **2016**, *48* (5), 629–634.
- (16) Yanuka, M.; Englman, R. Bond-Site Percolation: Empirical Representation of Critical Probabilities. *J. Phys. A. Math. Gen.* **1990**, 23 (7), L339.
- (17) Pekcan, Ö.; Yilmaz, Y.; Okay, O. In Situ Fluorescence Experiments to Test the Reliability of Random Bond and Site Bond Percolation Models during Sol-Gel Transition in Free-Radical Crosslinking Copolymerization. *Polymer* **1996**, *37* (11), 2049–2053.
- (18) Wang, R.; Lin, T.-S.; Johnson, J. A.; Olsen, B. D. Kinetic Monte Carlo Simulation for Quantification of the Gel Point of Polymer Networks. *ACS Macro Lett.* **2017**, *6*, 1414–1419.
- (19) Lang, M.; Müller, T. Analysis of the Gel Point of Polymer Model Networks by Computer Simulations. *Macromolecules* **2020**, *53* (2), 498–512.
- (20) Li, D. T.; Rudnicki, P. E.; Qin, J. Distribution Cutoff for Clusters near the Gel Point. ACS Polym. Au 2022, 2 (5), 361–370.
- (21) Lang, M. On the Elasticity of Polymer Model Networks Containing Finite Loops. *Macromolecules* **2019**, *52*, 6266–6273.
- (22) Yilmaz, Y.; Gelir, A.; Alveroglu, E.; Uysal, N. Testing Percolation Theory in the Laboratory: Measuring the Critical Exponents and Fractal Dimension during Gelation. *Phys. Rev. E* **2008**, 77 (5), 051121.
- (23) Adam, M.; Delsanti, M.; Munch, J. P.; Durand, D. Size and Mass Determination of Clusters Obtained By Polycondensation Near the Gelation Threshold. *J. Phys.* **1987**, *48* (10), 1809–1818.
- (24) Durand, D.; Delsanti, M.; Adam, M.; Luck, J. M. Frequency Dependence of Viscoelastic Properties of Branched Polymers near Gelation Threshold. *Europhys. Lett.* **1987**, 3 (3), 297–301.
- (25) Adam, M. Growth Process of Polymers Near the Gelation Threshold. *Makromol. Chem., Macromol. Symp.* **1991**, 45, 1–9.
- (26) Kaya, D.; Pekcan, Ö.; Yılmaz, Y. Direct Test of the Critical Exponents at the Sol-Gel Transition. *Phys. Rev. E* **2004**, *69* (1), 10.
- (27) Martin, J. E.; Wilcoxon, J.; Adolf, D. Critical Exponents for the Sol-Gel Transition. *Phys. Rev. A* **1987**, *36* (4), 1803–1810.
- (28) Winter, R.; Hua, D. W.; Song, X.; Mantulin, W.; Jonas, J. Structural and Dynamical Properties of the Sol-Gel Transition. *J. Phys. Chem. A* **1990**, 94 (6), 2706–2713.
- (29) Colby, R. H.; Rubinstein, M.; Gillmor, J. R.; Mourey, T. H. Scaling Properties of Branched Polyesters. 2. Static Scaling above the Gel Point. *Macromolecules* **1992**, *25*, 7180–7187.
- (30) Coniglio, A.; Stanley, H. E.; Klein, W. Site-Bond Correlated-Percolation Problem: A Statistical Mechanical Model of Polymer Gelation. *Phys. Rev. Lett.* **1979**, *42* (8), 518–522.
- (31) Rubinstein, M.; Colby, R. H. *Polymer Physics*; Oxford University Press: New York, 2003.
- (32) Kawamoto, K.; Zhong, M.; Wang, R.; Olsen, B. D.; Johnson, J. A. Loops versus Branch Functionality in Model Click Hydrogels. *Macromolecules* **2015**, *48*, 8980–8988.

- (33) Zhong, M.; Wang, R.; Kawamoto, K.; Olsen, B. D.; Johnson, J. A. Quantifying the Impact of Molecular Defects on Polymer Network Elasticity. *Science* **2016**, 353 (6305), 1264–1268.
- (34) Wang, J.; Lin, T.-S.; Gu, Y.; Wang, R.; Olsen, B. D.; Johnson, J. A. Counting Secondary Loops Is Required for Accurate Prediction of End-Linked Polymer Network Elasticity. *ACS Macro Lett.* **2018**, *7* (2), 244–249
- (35) Wang, R.; Alexander-Katz, A.; Johnson, J. A.; Olsen, B. D. Universal Cyclic Topology in Polymer Networks. *Phys. Rev. Lett.* **2016**, *116* (18), 188302.
- (36) Pine, D. J.; Weitz, D. A.; Chaikin, P. M.; Herbolzheimer, E. Diffusing Wave Spectroscopy. *Phys. Rev. Lett.* **1988**, *60* (12), 1134–1137.
- (37) Maret, G. Diffusing-Wave Spectroscopy. Curr. Opin. Colloid Interface Sci. 1997, 2 (3), 251–257.
- (38) Danielsen, S. P. O.; Beech, H. K.; Wang, S.; El-Zaatari, B. M.; Wang, X.; Sapir, L.; Ouchi, T.; Wang, Z.; Johnson, P. N.; Hu, Y.; Lundberg, D. J.; Stoychev, G.; Craig, S. L.; Johnson, J. A.; Kalow, J. A.; Olsen, B. D.; Rubinstein, M. Molecular Characterization of Polymer Networks. *Chem. Rev.* 2021, 121 (8), 5042–5092.
- (39) Beech, H. K.; Johnson, J. A.; Olsen, B. D. Conformation of Network Strands in Polymer Gels. *ACS Macro Lett.* **2023**, *12*, 325–330.
- (40) Matsunaga, T.; Sakai, T.; Akagi, Y.; Chung, U. Il.; Shibayama, M. SANS and SLS Studies on Tetra-Arm PEG Gels in as-Prepared and Swollen States. *Macromolecules* **2009**, *42* (16), 6245–6252.
- (41) Kovermann, M.; Saalwächter, K.; Chassé, W. Real-Time Observation of Polymer Network Formation by Liquid- and Solid-State NMR Revealing Multistage Reaction Kinetics. *J. Phys. Chem. B* **2012**, *116* (25), 7566–7574.
- (42) Spěváček, J. NMR Investigations of Phase Transition in Aqueous Polymer Solutions and Gels. *Curr. Opin. Colloid Interface Sci.* **2009**, *14* (3), 184–191.
- (43) Binauld, S.; Boisson, F.; Hamaide, T.; Pascault, J.-P.; Drockenmuller, E.; Fleury, E. Kinetic Study of Copper(I)-Catalyzed Click Chemistry Step-Growth Polymerization. *Polym. Sci. A Polym. Chem.* **2008**, *46*, 5506–5517.
- (44) Stanford, J. L.; Stepto, R. F. T.; Waywell, D. R. Rate Theory of Irreversible Linear Random Polymerisation. Part 2 Application to Intramolecular Reaction in A—A+ B—B Type Polymerisations. *J. Chem. Soc. Faraday Trans.* 1975, 71, 1308–1326.
- (45) Stanford, J. L.; Stepto, R. F. T. Rate Theory of Irreversible Linear Random Polymerisation. Part 1 Basic Theory. *J. Chem. Soc., Faraday Trans.* 1 1975, 71, 1292–1307.
- (46) Ahmad, Z.; Stepto, R. F. T. Approximate Theories of Gelation. Colloid Polym. Sci. 1980, 258 (6), 663–674.
- (47) Dutton, S.; Stepto, R. F. T.; Taylor, D. J. R. Monte-Carlo Modelling of the Formation, Structure and Properties of Polymer Networks. *Angew. Makromol. Chem.* **1996**, 240, 39–57.
- (48) Zhou, H.; Woo, J.; Cok, A. M.; Wang, M.; Olsen, B. D.; Johnson, J. A.; Weitz, D. A. Counting Primary Loops in Polymer Gels. *Proc. Natl. Acad. Sci. U.S.A.* **2012**, *109* (47), 1919–19124.
- (49) Lin, T.-S.; Wang, R.; Johnson, J. A.; Olsen, B. D. Topological Structure of Networks Formed from Symmetric Four-Arm Precursors. *Macromolecules* **2018**, *51* (3), 1224–1231.
- (50) Nishi, K.; Fujii, K.; Katsumoto, Y.; Sakai, T.; Shibayama, M. Kinetic Aspect on Gelation Mechanism of Tetra-Peg Hydrogel. *Macromolecules* **2014**, 47 (10), 3274–3281.
- (51) Pereda, S.; Brandolin, A.; Valles, E. M.; Sarmoria, C. Copolymerization Between A3 and B2 with Ring Formation and Different Intrinsic Reactivity in One of the Monomers. *Macromolecules* **2001**, *34*, 4390–4400.
- (52) GitHub Repository, https://github.com/olsenlabmit/forward_reverse_gel_point.
- (53) Spouge, J. L. Equilibrium Ring Formation in Polymer Solutions. *J. Stat. Phys.* **1986**, 43 (1–2), 143–196.
- (54) Gordon, M.; Scantlebury, R. Statistical Kinetics of Polyesterification of Adipic Acid with Penta-Erythritol or Trimethylol Ehtane. *J. Chem. Soc. B* **1967**, *1*, 1–13.

- (55) Cail, J. I.; Stepto, R. F. T. The Gel Point and Network Formation Theory and Experiment. *Polym. Bull.* **2007**, *58* (1), 15–25.
- (56) Tanaka, Y.; Stanford, J. L.; Stepto, R. Interpretation of Gel Points of an Epoxy-Amine System Including Ring Formation and Unequal Reactivity: Reaction Scheme and Gel-Point Prediction. *Macromolecules* **2012**, 45 (17), 7186–7196.
- (57) Wang, R.; Alexander-Katz, A.; Johnson, J. A.; Olsen, B. D. Universal Cyclic Topology in Polymer Networks. *Phys. Rev. Lett.* **2016**, *116* (18), 1–5.
- (58) Schwartz, D.; Steinberg, S. Scaling of Kinetically Growing Clusters. *Phys. Rev. Lett.* **1992**, *51* (13), 1123–1126.
- (59) Meakin, P. Diffusion-Controlled Cluster Formation in 2 6-Dimensional Space. *Phys. Rev. A* **1983**, 27 (3), 1495–1507.
- (60) Gupta, A. M.; Hendrickson, R. C.; Macosko, C. W. Monte Carlo Description of Af Homopolymerization: Diffusional Effects. *J. Chem. Phys.* **1991**, 95 (3), 2097–2108.
- (61) Lin, T. Towards Quantitatively Predicting the Properties of Gels and Elastomers; 2021.
- (62) Zhou, H.; Schön, E.-M.; Wang, M.; Glassman, M. J.; Liu, J.; Zhong, M.; Díaz Díaz, D.; Olsen, B. D.; Johnson, J. A. Crossover Experiments Applied to Network Formation Reactions: Improved Strategies for Counting Elastically Inactive Molecular Defects in PEG Gels and Hyperbranched Polymers. *J. Am. Chem. Soc.* **2014**, *136*, 9464–9470.